

Dillenia indica bark extract mediated bio-fabrication of copper nanoparticles: characterisation, antioxidant and anticancer activity *in vitro*

Larica Mohanta^{a,b} and Bhabani Sankar Jena^{a,b}

^aCSIR-Institute of Minerals and Materials Technology, Bhubaneswar, India; ^bAcademy of Scientific and Innovative Research (ACSIR), Ghaziabad, India

ABSTRACT

Dillenia indica is a medicinal plant used in the indigenous system of medicine for plethora of diseases. In this study, the efficacy of ethanolic bark extract of *Dillenia indica* was investigated for green synthesis of copper nanoparticles (CuNPs). Obtained CuNPs were crystalline, spherical in shape within a size range of 20.87–45.73 nm, well dispersed showing strong negative zeta potential value (−41.8 mV) as analysed by XRD, TEM, FESEM and particle size analyser. The elemental composition of CuNPs was examined through EDX spectrum followed by field map analysis. FTIR spectra showed the presence of active biomolecules responsible for reduction of copper ions as well as for surface functionalisation of CuNPs. Synthesised CuNPs showed marked free radical scavenging efficacy at IC₅₀ of 37.2 µg/mL. MTT assay in CuNPs treated A549 and MCF-7 cancer cell lines for 24 and 48 h showed substantial decrease of cell viability with increase in concentration. Further, morphological alterations like cell shrinkage, nuclear fragmentation and blebbing were remarkably observed in CuNPs treated both the cell lines as assayed through AO/EtBr and DAPI staining methods. Thus, *D. indica* bark extract-mediated CuNPs were potential free radical scavengers and effective cytotoxic against A549 and MCF-7 cancer cell lines.

ARTICLE HISTORY

Received 11 April 2023
Accepted 11 August 2023


KEYWORDS

Green synthesis; *Dillenia indica*; copper nanoparticles; antioxidant; anticancer

1. Introduction

In recent years' nanotechnology circumscribed an increasing impact on industrial and medical research accounting to find solutions across a wide range of physicochemical and biomedical science. Development of different inorganic and organic nanomaterials exhibit completely different properties, as they have distinct features including distribution, size and shape which act as crossroads of multiple applications in biotechnology including

CONTACT Bhabani Sankar Jena  bsjena@immt.res.in CSIR-Institute of Minerals and Materials Technology, Bhubaneswar-751013, Odisha, India

 Supplemental data for this article can be accessed online at <https://doi.org/10.1080/17458080.2023.2249241>.

This article has been corrected with minor changes. These changes do not impact the academic content of the article.
© 2023 The Author(s). Published by Informa UK Limited, trading as Taylor & Francis Group.

This is an Open Access article distributed under the terms of the Creative Commons Attribution License (<http://creativecommons.org/licenses/by/4.0/>), which permits unrestricted use, distribution, and reproduction in any medium, provided the original work is properly cited. The terms on which this article has been published allow the posting of the Accepted Manuscript in a repository by the author(s) or with their consent.

tissue engineering, drug delivery, imaging, diagnostics, electronics, textile and food packaging industries [1].

The scientific community has customised many suitable synthesis techniques for the production of nanoparticles according to their applications. However, various physico-chemical approaches for the synthesis of metal nanoparticles have their disadvantages, such as the use of hazardous chemicals as reducing agents, expensive and time-consuming process [2]. Green nanotechnology has become a new trend in nanoparticle production due to its several advantages such as eco-friendly, reproducibility in production, easy scaling-up and less expensive [3]. In this regard, several biological reducing agents such as plants (extracts of the whole plant, plant parts and plant derived phytochemicals), microorganisms (bacteria, fungi, yeast and algae) and biomolecules (proteins, carbohydrates and nucleic acids) are used for nanomaterial synthesis. Among these, plant-mediated nanoparticle production has been regarded as an economical, stable and environmentally friendly technology [4,5].

Among various metal nanoparticles, copper nanoparticles (CuNPs) have received a lot of attention in the domains of nanotechnology and nanomedicine over last ten years, because of being more economical to be utilised efficiently in catalytic, sensors, optical, electrical, agricultural and biomedical applications [6]. Copper is an effective trace element involved in the nutrition system of living organism [7]. The unique properties of CuNPs, such as high surface to volume ratio, ductility, strength and yield makes it a potentially cost-efficient nanomaterial to be used in various therapeutic applications, such as catalytic, antioxidant, antimicrobial, antifungal and cytotoxic activities [8]. The thermal reduction, laser ablation, microemulsion, polyol method, etc., have been used for production of CuNPs [9]. However, due to ease-of-use and environmental compatibility, the biological production of CuNPs employing plants as bio reducers has been studied to overcome the restrictions occurred due to physical and chemical methods.

Dillenia indica L. (commonly known as elephant apple) belongs to family Dilleniaceae is a medicinal plant found in sub-Himalayan region of tropical Asian continent. As reported, extracts from plant parts have extraordinary properties like antidiabetic [10], antioxidant [11], antimicrobial, anticancer properties [12], etc. It contains host of secondary metabolites like lupeol, betulinaldehyde, betulinic acid, myricetin, sitosterol and stigmasterol [12] which helps in synthesising biocompatible CuNPs with greater stability. Mohanty and Jena [13] have reported the free radical scavenging activity of *D. indica* bark extract which was further used for synthesis of AgNPs.

The need of searching most effective and appropriate drugs for treatment of cancer has been evolved as a challenging task in recent years because of increasing number of cancer deaths. The use of chemotherapy, radiation therapy, cancer-related drugs for treatment of cancer also affects normal cells leading to neuron damage and skin problems [14]. Hence, there is an urgent requirement for development of potent, cost-effective cancer treatment method for the benefit of mankind.

In the last 10 years, lung cancer has emerged as a dreadful disease-causing million of deaths worldwide. It was evaluated that near about 1.6 million deaths has occurred through lung cancer worldwide in 2012 [15]. Similarly, breast cancer is most common in case of females which accounts for 1 in 3 of each new females every year. Lung's cancer is the leading cause of death in men and second highest in women (after breast cancer) [16]. The main cause of lung cancer is attributed to increased intake of tobacco and smoking which causes nearly 30% of all deaths [17]. Other environmental factors causing cancer are absorption of UV-radiation, occupational exposure to organic and inorganic substances, infectious microorganism, obesity, hormonal therapy (breast cancer), air and water pollution. The rise of cancer over time has challenged the researchers to find out new, favourable and environment-friendly cancer remedies.

Singh et al. [18] studied the *in vitro* anticancer activity of green synthesised AgNPs using leaf extract of *Carissa carandus* against hepatic (HUH-7) and renal (HEK-7) cell lines. Synthesis of AgNPs using endophytic fungi *Botryosphaeria rhodina* exerts cytotoxic properties on A549 cell lines through radical scavenging and apoptosis [19]. The findings suggested that the active biomolecules present in the fungi may be responsible for the cytotoxic activity of AgNPs in *in vitro* conditions. Similarly, concentration-dependent cytotoxicity of enterococcus-mediated AuNPs against human colorectal cancer cells (HT-29) was observed by Vairavel et al. [20]. Morphological changes occurring due to apoptosis were also observed. Shwetha et al. [21] prepared ZnONPs using *Areca catechu* extract as reducing agent attributes potential cytotoxicity against MCF-7 cell line.

A study by Valodkar et al. [22] on biosynthesised CuNPs using medicinal plant *Euphorbia nivulia* L. has indicated biological consequences on tumour cells. *In vitro* anticancer activity of *Eclipta prostata* leaf extract mediated synthesis of CuNPs was demonstrated by Chung et al. [23] against HepG2 cell lines. CuONPs also exhibited anticancer potency against HeLa cell lines in concentration-dependent manner [24]. Manikandan et al. [25] bio-fabricated CuONPs using leaf extract of *Ocimum americanum* which showed potent cytotoxic activity in A549 cancer cell lines. Hasanin et al. [26] observed the cytotoxic activity of CuNPs-starch nanocomposites against breast cancer cell lines.

This study was focused on green synthesis of CuNPs using ethanolic bark extract of *Dillenia indica* as reducing as well as stabilising agent. The synthesised CuNPs were characterised using different physicochemical characterisation techniques. Evaluation of free radical scavenging activity of CuNPs was done using 2,2-diphenyl-1-picrylhydrazyl (DPPH) assay. The cytotoxic ability of biosynthesised CuNPs was studied against human lung cancer (A549) and breast cancer (MCF-7) cell lines. This report provides comprehensive details regarding biosynthesis, antioxidant and anticancer activities of CuNPs which will have a remarkable impact on biomedical applications.

2. Materials and methods

2.1. Chemicals

Copper chloride ($\text{CuCl}_2 \cdot 2\text{H}_2\text{O}$) and diphenyl-picryl hydrazine (DPPH) were procured from Himedia, Mumbai. All chemicals and solvents were purchased from Merck in Mumbai, India. 3-(4, 5-Dimethylthiazol-2-yl)-2,5-diphenyltetrazolium bromide (MTT), DAPI, Dulbecco's Modified Eagle Media (DMEM), dimethyl sulfoxide (DMSO) and fetal bovine serum (FBS) were purchased from Sigma-Aldrich company of USA.

2.2. Preparation and extraction of *D. indica* bark extract

Extraction and preparation of *D. indica* bark extract was done according to Mohanty and Jena [13] with some minor modifications. The trunk barks were collected from an age-old *D. indica* plant in CSIR-IMMT Campus, Bhubaneswar, Odisha, India followed by proper washing to remove dirt. These were allowed to dry for 4d and grounded to fine powder (mesh size 60). Extraction of nonpolar compounds was done by dissolving 100g of bark powder in 1L of hexane for 6h. Further, the dried powder was dissolved in 80% ethyl alcohol in order to extract highest number of polyphenols. The extraction was repeated twice followed by filtration using Whatman No. 41 filter paper. The required bark extract was obtained by concentrating the solvent in a rotary vacuum evaporator at 45°C and was stored at 4°C for further use.

2.3. Phytochemical screening test

The qualitative screening analysis was done to establish the presence of several active phytoconstituents, such as phenols, flavonoids, alkaloids, steroids, terpenoids in the ethanolic bark extract of *D. indica*. The analysis was done according to the standard protocols reported [27–29].

2.4. Synthesis and optimisation of CuNPs using ethanolic bark extract of *D. indica*

Copper nanoparticles were synthesised by adding bark extract (2 mg/mL) dissolved in aqueous medium to $\text{CuCl}_2 \cdot 2\text{H}_2\text{O}$ solution (1 mM) following adjustment of pH to 10 by adding 10 mM NaOH. The reaction mixture was heated to 60 °C in a hot water bath for 15 min. The formation of CuNPs was confirmed by the appearance of wine-red colouration. The coloured mixture was centrifuged at 12,000 rpm for 20 min and obtained pellet was washed thrice with distilled water to remove any unbound biological molecules followed by drying at hot air oven to obtain fine powder which was used for further analysis. However, the synthesis of CuNPs was optimised by considering the effect of different reaction parameters such as concentration of copper salt (0.1, 1 and 10 mM), concentration of bark extract (1, 2 and 4 mg/mL), temperature (50, 60, 80 and 90 °C) and pH (4, 7, 10, 11 and 12) of the medium.

2.5. Characterisation of CuNPs

The synthesis of CuNPs was monitored between 300 and 800 nm and measured in UV–visible spectrophotometer (Eppendorf Biospectrometer, Hamburg). Synthesised nanoparticle solution was stored at ambient temperature. The stability of CuNPs was monitored by UV spectral analysis for up to one month. The structural morphology and size of the nanoparticles were obtained from a TEM (FEI Tecnai G2 20, Eindhoven, Netherlands) analyser. The CuNPs solution was sonicated for 10 min at 40 kHz prior to analysis using ultrasonic homogeniser for proper dispersion (Model 3000 MP, Biologics, Manassas, VA). On the carbon-coated copper grid, a drop of the CuNPs solution was poured, and dried under a lamp for one hour. Particle size distribution and Zeta potential of synthesised CuNPs were analysed using a Dynamic light scattering (DLS) unit (Anton Paar Litesizer 500). Sample was prepared with 20 μL of synthesised CuNPs in 1 mL of deionised water. Chemical composition and structural analysis were conducted using EDX analyser associated with field emission scanning electron microscope (FESEM–Jeol JSM-IT 800, Tokyo, Japan and EDX–Elect Super, AMTEX, USA). The XRD pattern of CuNPs was obtained using X'pert PRO X-ray diffraction unit (PANalytical, Almelo, Netherland) within the diffraction angle between 10° and 90° (2Θ). The FT-IR spectra of the *D. indica* bark extract and CuNPs were obtained by using Bruker Alfa II spectrophotometer in the transmittance range between 4000 and 500 cm^{-1} to identify the surface functional groups which are capable of reduction and formation of CuNPs.

2.6. Free radical scavenging activity

The antioxidant potential of *D. indica* bark extract, CuCl_2 and biosynthesised CuNPs were determined by DPPH assay [30]. Different concentrations of extract, CuCl_2 and CuNPs (25, 50, 100 and 200 $\mu\text{g/mL}$) were prepared in order to assess the potential to scavenge the DPPH radicals. The volume of each tube was made up to 0.5 mL by

methanol. 0.1 mM DPPH solution (5 mL) was added to these tubes and thoroughly vortexed. The tubes were incubated for 20 min at room temperature in dark and absorbance was measured at 517 nm against methanol blank. DPPH in methanol without test sample was treated as control. The free radical scavenging capacity of *D. indica* bark extract was compared with BHA (butylated hydroxy anisole) standard. The antioxidant potency of *D. indica* bark extract, CuCl_2 and CuNPs was calculated by the standard equation:

$$\% \text{ Radical Scavenging Activity} = (\text{Control OD} - \text{Sample OD}) / \text{Control OD} \times 100$$

2.7. Cytotoxic activity of CuNPs: in vitro

2.7.1. Cell culture

A549 (Adenocarcinoma human alveolar basal epithelial) and MCF-7 (breast cancer) cell lines were obtained from Imgenex, Bhubaneswar, India. The cells were kept in an incubator at 37°C with a supply of 5% CO_2 and were nourished with DMEM containing 10% FBS and 1% antibiotic-antimycotic solution. For all experiments, cells were seeded to produce an experimental stage of 80% confluency in cell culture flasks or well plates. The flasks/plates were observed under a phase contrast inverted microscope (Leica DM IL LED, Germany) to detect morphological changes and photographed using a camera.

2.7.2. Cell viability assay

Effect of synthesised copper NPs, copper chloride and extract on cell proliferation was evaluated using MTT assay. The tests were conducted on white corning 96-well plates (Corning, Costar, New York, NY). In this investigation, cells were seeded in a 96-well plate at a density of 1×10^5 cells per well prior to the experiment and maintained in a CO_2 incubator at 37°C and 5% CO_2 for 24 h. Following 24 h growth, the medium was changed with fresh media and the cells were treated with eight different concentrations of synthesised NPs (30–240 $\mu\text{g}/\text{mL}$) for 24 and 48 h. Well-containing cells without any treatment were used as negative control and metal salt solution (1 mM) and *D. indica* bark extract (2 mg/mL) as used for synthesis of CuNPs were included as positive controls. After 24 and 48 h, 20 μL of MTT solution (5 mg/mL) was added to each well. Then, the plates were allowed for an additional 4 h for reduction of MTT to formazan at 37°C till the formation of purple-coloured formazan. After incubation period, media was discarded and washed with PBS. To dissolve the formazan crystal, 100 μL of MTT solubilisation solution (DMSO) was administered to each well. The absorbance of 96 well plates was measured at 490 nm by using a micro plate reader (iMARK TM Micro Plate Reader, Bio-Rad Laboratories Inc., Hercules, CA).

2.7.3. Dual fluorescent dye (AO/EtBr) staining

Nuclear staining using acridine orange/ethidium bromide (AO/EtBr) dual fluorescent stain, was used to analyse the apoptosis in A549 and MCF-7 cell lines (1×10^5). The cells were treated separately with CuNPs (240 $\mu\text{g}/\text{mL}$), CuCl_2 (1 mM) and extract (2 mg/mL) solution separately in 6-well plates and incubated for 24 h. After overnight incubation, the cells were given a mixture containing 20 μL of AO/EtBr staining solution in 1:1 ratio (100 $\mu\text{g}/\text{mL}$ in PBS). After 5 min, the cells were visualised under fluorescence microscope (Leica, DM3000). Based on the emission of green, orange and red fluorescence for live, apoptotic and necrotic cells, respectively, the treated cells were separated from one another.

2.7.4. Assessment of nuclear damage by DAPI staining

In this study, the cyto-morphological changes in the nuclei of control and treated MCF-7 and A549 cells were assessed using the DAPI (4', 6-diamidino-2-phenylindole) stain. This staining method was done according to [31] with slight modifications. Cells were treated with CuNPs (240 µg/mL), CuCl₂ (1 mM) and extract (2 mg/mL) for 24 and 48 h in a humidified atmosphere of 5% CO₂ at 37°C. After incubation cells were gently scraped and harvested by centrifugation. The cells were fixed for 10 min at room temperature with 4% paraformaldehyde, and then mounted with DAPI (2.5 g/mL). The morphological changes were observed using fluorescence microscopy (Leica, DM3000).

2.8. Statistical analysis

All the data obtained were statistically analysed using GraphPad Prism version 8 software (Graphpad Software Inc., La Jolla, CA). An analysis of variance (ANOVA) followed by Tukey's post-hoc test was used for multiple comparison of samples. Values depicting $p < 0.05$ were considered statistically significant between the treated and control groups. Experiments were carried out in triplicate and the results were expressed as mean \pm standard error of mean (SEM).

3. Results and discussion

3.1. Phytochemical screening analysis

Plant extract acts as an efficient substitute for reducing and capping agents due to the presence of various bioactive compounds like phenols, flavonoids, terpenoids, steroids, glycosides, tannins, etc. The present phytochemical screening of ethyl alcoholic extract of *D. indica* indicated the presence of phenolics and flavonoids as the major constituents in addition to saponins, alkaloids, steroids and tannins which corroborates with the results obtained by Deepa and Jena [11] (Table 1). Reports on different plants also specified the presence of the above compounds involved in reduction and stabilisation of metal and oxides nanoparticles. Weng et al. [32] observed the presence of flavonoids, alkaloids and chlorophyll in the leaf extract of *Eucalyptus* which work as a reducing and capping agent for synthesis of Fe and AgNPs.

3.2. Role of phytoconstituents in reduction and stabilisation of CuNPs

Plant phytoconstituents play a major role in the reduction and capping of metal's nuclei for production of nanoparticles. The bark of *D. indica* L. contains phytochemicals like betulinaldehyde, betulinic acid, betulin, lupeol, myricetin and dillenetin [12]. As

Table 1. Qualitative screening analysis of *D. indica* bark extract.

Sl. No.	Secondary metabolites	Test	Observation	Results
1	Phenols	Ferric chloride test	Bluish black or violet	++
2	Flavonoids	Alkaline reagent test	Intense yellow or orange	++
3	Alkaloids	Mayer's test	Yellow	+
4	Tannins	Lead acetate test	White turbid	+
5	Saponins	Froth test	Appearance of foam	-
6	Terpenoids	Salkowski test	Reddish brown	-
7	Steroids	Salkowski test	Red colour in upper layer	+

mentioned, the qualitative screening showed the presence of various secondary metabolites, such as phenols, tannins, alkaloids, flavonoids, saponins with phenols and flavonoids as highest concentration. The functional groups of these phytochemicals are carboxylic, alkanes, aromatic rings, hydroxyl and carbonyl having key role in the reduction of copper ion to formation of CuNPs of controlled shape and size.

For possible mechanism in the synthesis CuNPs in this study, we propose the role of myricetin one among the various biomolecules present in *D. indica*. It is hypothesised that the reactive hydrogen atom from myricetin is released during tautomeric transformation reaction of the enol form to keto form which helps in reduction of copper ions to generate CuNPs (Figure 1). The divalent or monovalent valence states of copper metal ion are transformed to zero-valence state copper nuclei during the synthesis process. Further, these nuclei combine to form CuNPs of various forms in nucleation process [33].

3.3. Biosynthesis of CuNPs

Biogenic synthesis of nanoparticles using plant as reducing agents gains advantages over other biomaterials because of being cost effective, easy availability, safe handle, easy scale up, etc. In this context, a single step process was achieved for synthesis of CuNPs using ethanolic bark extract of *Dillenia indica* which reduces Cu^{2+} ion of copper chloride solution to Cu^0 . The main factor used to support the synthesis of CuNPs was the colour change of the reaction mixture, which was observed using UV-visible spectroscopy. Addition of bark extract to CuCl_2 solution changes the colour of the reaction mixture from light yellowish to wine red indicating the formation of CuNPs (Figure 2). Changing of the colour of reaction mixture is attributed to surface Plasmon resonance (SPR) phenomenon.

3.4. Optimisation of reaction parameters on synthesis of CuNPs

The synthesis procedure of CuNPs was optimised by taking consideration of variables like concentrations of *D. indica* bark extract (1, 2 and 4 mg/mL), concentration of metal salt

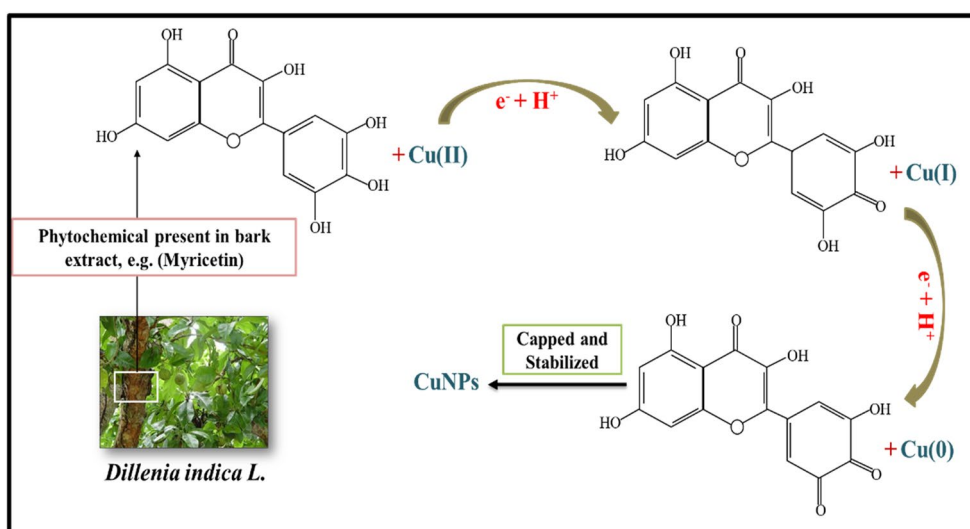


Figure 1. Plausible reduction mechanism of copper metal into CuNPs by *Dillenia indica* bark extract.

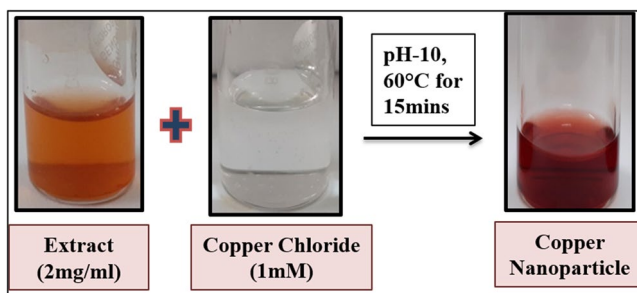


Figure 2. Synthesis of CuNPs using ethanolic bark extract of *Dillenia indica*.

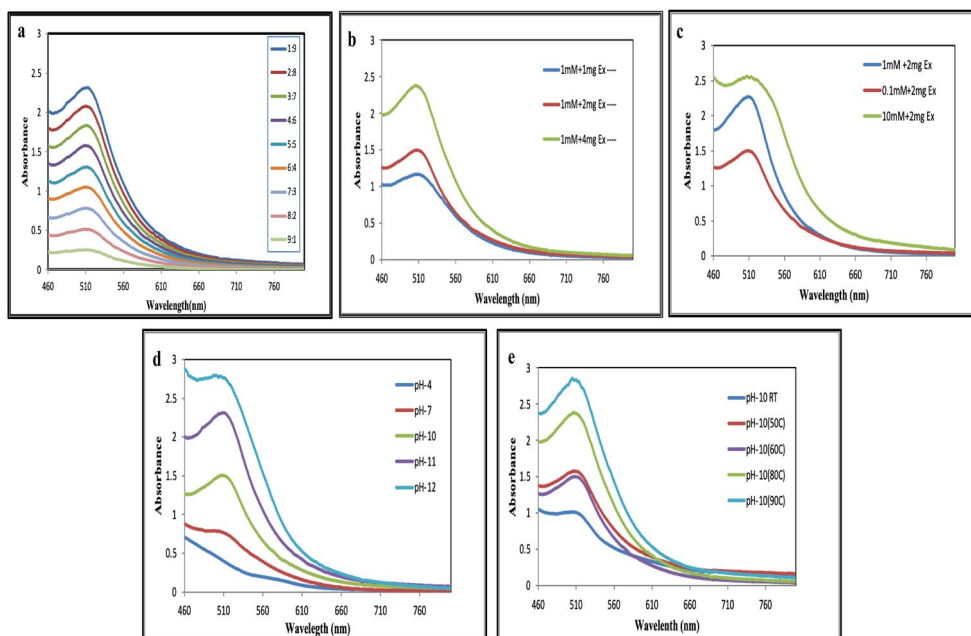


Figure 3. Optimisation of CuNPs synthesis parameters: (a) Mixing ratio of extract and CuCl_2 , (b) concentration of bark extract, (c) molarity of copper chloride, (d) effect of pH and (e) effect of temperature.

solution (0.1, 1 and 10 mM), mixing ratio of bark extract and salt solution, pH (4, 7, 10, 11 and 12) and temperature (40, 50, 60, 80 and 90°C).

The amount of bark extract used performs a significant role in the transformation of metal ions into nanoparticles. The mixing ratio of bark extract with CuCl_2 solution in the synthesis process has been measured by UV-visible spectrophotometer (Figure 3(a)). The data revealed that the strength of the SPR peak increases with increase in the ratio of bark extract up to 1:9. However, analysis through TEM it was found that the CuNPs were agglomerated at ratio 1:9 (Figure S1) hence, the optimal level at a ratio of 1:4 (CuCl_2 : Extract) was taken into consideration for this study. The reactions were conducted at pH 10.

Similarly, the concentration of bark extract was examined at 1, 2 and 4 mg/mL which showed increase in the intensity of SPR peak as illustrated in Figure 3(b). However, at

higher concentration (4mg/mL) the absorbance peak becomes progressively broader. Thus, increasing the concentration of bark extract leads to agglomeration of CuNPs as visualised through TEM (Figure S2) which may be due to presence of excessive biomolecules present in the extract initiating secondary reaction on the surface of nuclei, thus increasing the particle size [34]. Therefore, the optimal concentration of bark extract was 2mg/mL for synthesis of CuNPs [34].

The effect of precursor salt concentration on the formation of CuNPs was studied between 0.1, 1 and 10 mM CuCl₂ solution (Figure 3(c)). Optimisation of initial concentration of metal salt is required in order to obtain smaller-sized NPs with desired shape. This analysis showed that an increase in the concentration of CuCl₂ from 0.1 to 1 mM leads to formation of smaller-sized CuNPs without agglomeration but further increasing the concentration yields large sized and agglomerated CuNPs. A similar outcome was reported using *Azadiracta indica* leaf extract for the reduction of copper ions [34]. Therefore, the optimum precursor salt concentration for synthesis of CuNPs was 1 mM.

Another important parameter for synthesis of metal NPs is the pH of the reaction mixture. Variation in pH affects morphology and stability of the NPs. In this study of nanoparticle synthesis, simply mixing of bark extract to CuCl₂ solution did not lead to the formation of CuNPs. However, after altering the pH of the medium from acidic to alkaline by adding 10 mM NaOH, CuNPs were obtained (Figure 3(d)). These findings were further supported by Kiruba Daniel et al. [35] who synthesised CuNPs using leaf extract of *Dodonaea viscosa* for obtaining spherical-shaped CuNPs at pH 10. The importance of pH for synthesis of CuNPs was also reported [36]. At pH 4 no absorbance peak was observed and the colour of the solution was yellow. Increasing the pH to 10 and 11 colour changes to deep red and absorbance peak was observed at 512 nm and 510 nm. At pH 12 the absorbance peak broadens and agglomeration of CuNPs was observed due to presence of impurities and unbound particles such as Cu₂O, Cu (OH)₂. Therefore, in this study optimum pH for synthesis of CuNPs was established at pH 10.

The effect of temperature also plays an important role influencing the synthesis process of CuNPs. It was observed that the rate of conversion of Cu²⁺ ions to Cu⁰ increased considerably by varying temperature range from 40 to 90 °C, but the synthesis rate increased up to 60 °C (Figure 3(e)). At higher temperature, agglomeration and large-sized CuNPs were formed containing impurities as observed in TEM analysis (Figure S3). Therefore, the optimum temperature of the reaction medium for synthesis of CuNPs was established at 60 °C. Reports showed optimisation and synthesis of CuNPs at 60 °C using *Dodonaea viscosa* extract as bioreductant [35].

Therefore, the reaction mixture containing 2 mg/mL of *D. indica* bark extract dissolved in aqueous medium was added to 1 mM CuCl₂ · 2H₂O at pH 10 and kept in a hot water bath for 15 min at 60 °C was considered to be the optimum synthesis conditions for CuNPs as monitored by UV–visible spectrophotometer.

3.5. Characterisation of synthesised CuNPs

In this study, we report a cost-effective, eco-friendly and easy procedure for the synthesis of the CuNPs using ethanolic bark extract of *Dillenia indica* L. as a reducing and capping agent. The biosynthesis of CuNPs was preliminarily confirmed by UV–visible spectrophotometer. The CuNPs obtained were characterised by Particle Size Analyser, TEM and FTIR and were found to be stable for one month.

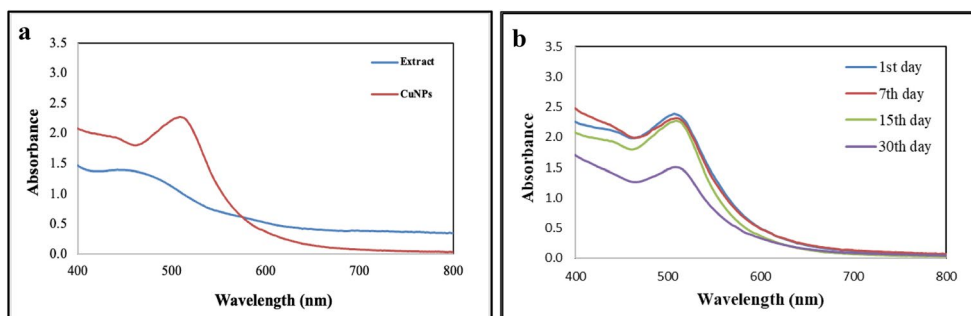


Figure 4. UV-visible absorption spectra of (a) biosynthesised CuNPs and *D. indica* bark extract and (b) CuNPs between 1 and 30 d.

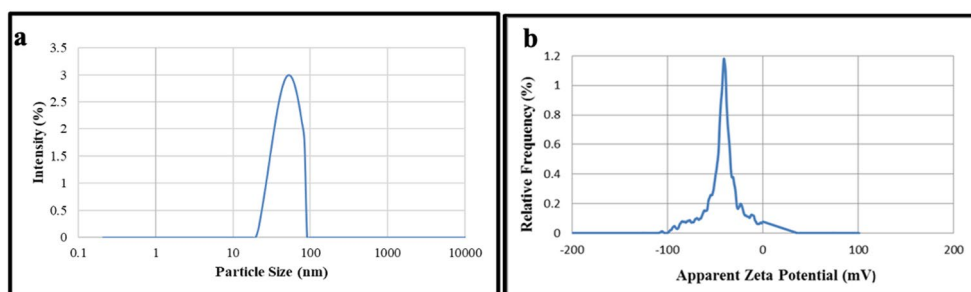


Figure 5. Particle size distribution (a) and Zeta potential analysis (b) of CuNPs.

3.5.1. UV-visible spectroscopic analysis

A UV-visible spectrophotometer was used to examine the synthesis of CuNPs obtained by reducing metal ions using *D. indica* bark extract as bioreducer. The formation of CuNPs was indicated by the appearance dark wine-red colour with maximum wavelength of 512nm due to vibrations in SPR and reduction of copper chloride ions by *D. indica* bark extract (Figure 4(a)). As per reports, the absorption bands for CuNPs were found in the range of 500–600nm [37]. The absorbance peak of *D. indica* bark extract was observed at 440nm. Production of CuNPs occurs due to the presence of active biomolecules from bark extracts which were mostly accountable for reduction of Cu^{2+} ions. The synthesised CuNPs were found to be stable for up to one month with no change in the position and symmetry of the absorption peak which depicts capping of phytoconstituents of *D. indica* extract on the surface of NPs thereby protecting it from agglomeration and decomposition (Figure 4(b)). CuNPs synthesised using *Euphorbia prolfifera* leaf extract were also quite stable up to one month with no significant difference in the position of absorption peak [38].

3.5.2. Particle size analyser

The particle size distribution of synthesised CuNPs was measured using DLS unit. The particles formed were monodisperse with average particle size of 54nm (Figure 5(a)). CuNPs' polydispersity index (PDI) was found to be 0.33 which showed that the NPs were evenly scattered in water. The amount of electrostatic repulsion between neighbouring and similarly charged particles in the dispersion is indicated by the value of zeta potential. Higher stability of NPs is indicated by the large magnitude of the zeta potential value [34]. The average zeta potential value of synthesised CuNPs has been found at -41.8mV (Figure

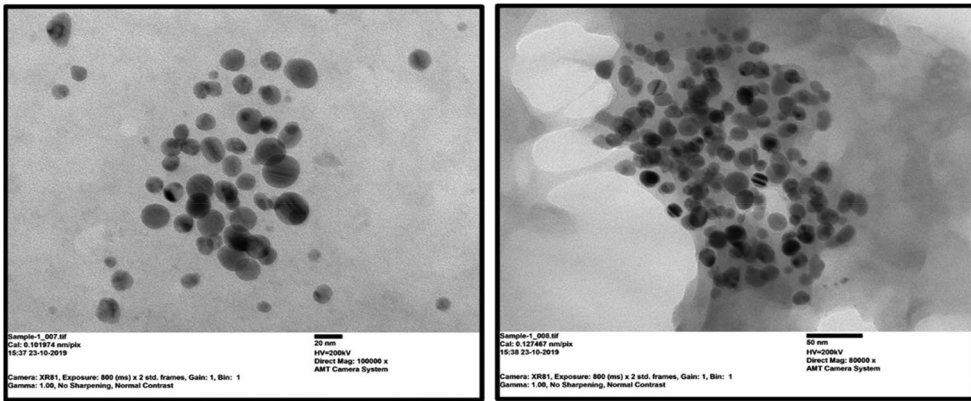


Figure 6. Transmission electron microscopy image of CuNPs (well-dispersed and spherical) synthesised using *D. indica* bark extract.

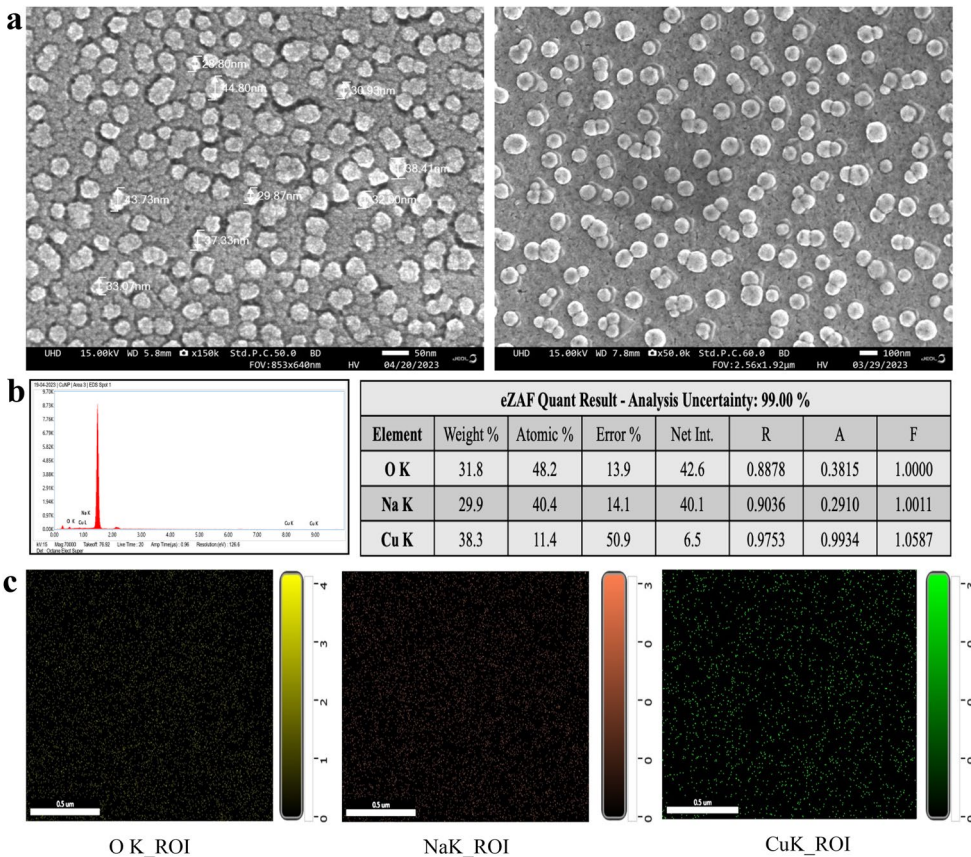


Figure 7. (a) Field emission scanning electron microscopy image, (b) Energy dispersive X-ray (EDX) analysis and (c) elemental mapping analysis of biosynthesised CuNPs.

5(b)) suggesting highly stable CuNPs. The -ve zeta potential value was may be due to the phenolics compounds present in the bark extract acting as capping agent for NPs which also contributed for their stability as seen in UV-visible spectrophotometric study for one

month. We have also obtained high level of positivity of phenolics in the extract during phytochemical screening (Table 1). Moreover, monodisperse CuNP provides a useful attribute for material scientists to improve biomedical applications associated with CuNPs.

3.5.3. TEM analysis

Transmission electron microscopy analysis provided further insight into the shape, size and aggregation of *D. indica* mediated CuNPs. The TEM micrograph (Figure 6) revealed monodispersed, spherical-shaped CuNPs without agglomeration. The size distribution of CuNPs was between 5 and 30 nm. Similar results were also observed from TEM micrographs of CuNPs synthesised using *Dodonaea viscosa* leaf extract with size ranging between 30 and 40 nm exhibiting spherical shape [35]. According to Chung et al. [23] CuNPs were biosynthesised using *Eclipta prostrata* leaf extract, and TEM investigation showed that the NPs were spherical in form with size varying from 28 to 45 nm.

3.5.4. FESEM and EDX analysis

The field emission scanning electron microscopy (FESEM) was employed to assess the surface morphology of biosynthesised CuNPs whereas Energy-dispersive X-ray spectrometry (EDX) analysis was conducted to confirm the presence of copper element in synthesised CuNPs. FESEM images showed that CuNPs had spherical morphology with an approximately uniform distribution, and their sizes ranged from 20.87 to 45.73 nm with a mean particle size of 35.43 nm (Figure 7(a)). Earlier investigations on synthesised CuNPs using herbal extract have reported different size of NPs ranged from 5 to 100 nm [39].

The EDX analysis of synthesised CuNPs confirmed the presence of Cu element with weight percentage of Cu as 38.3% (Figure 7(b)). This includes distinguishable absorption peaks at 1.00, 8.00 and 9.00 keV which are specific to Cu metal [40]. The results correlate with several other studies reported previously [39,41]. Apart from Cu, EDX spectra showed the existence of Na (29.9%), O (31.8%) and C which might be due to involvement of phytochemicals of *D. indica* extract in the reduction and capping of CuNPs [40]. In addition, EDX analysis was carried out in field map analyses of the elements (Figure 7(c)). However, the existence of a large number of oxygen atoms suggested that biocomponents were using oxygen atoms to bind the CuNPs [23,42].

3.5.5. XRD analysis

The crystalline nature of biosynthesised CuNPs was determined using the XRD technique. Bragg's reflections with 2θ values of 40.51° , 45.52° , 66.38° and 75.32° corresponding to

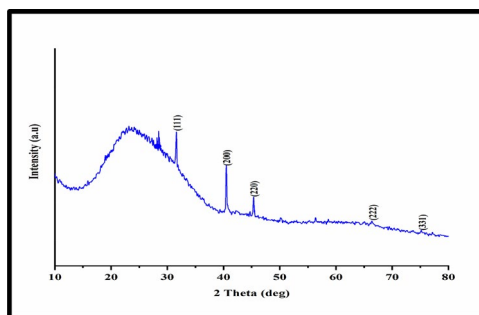


Figure 8. XRD pattern of Phytosynthesised CuNPs.

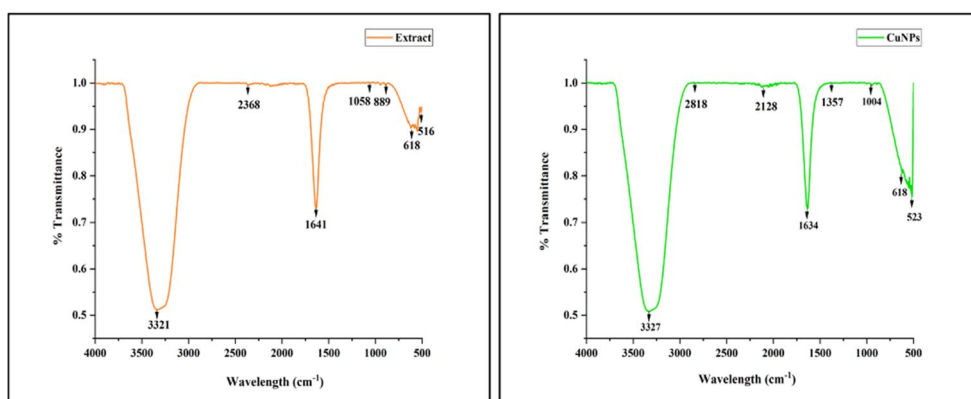


Figure 9. FTIR spectra of synthesised CuNPs and *D. indica* bark extract.

Table 2. Functional groups present on the surface of biosynthesised CuNPs in comparison to that present in bark extract.

Functional group	<i>D. indica</i> bark extract (cm ⁻¹)	CuNPs (cm ⁻¹)
O-H	3321	3327
-C-H-	-	2818
-C-H-	2368	2128
-C=C-	1641	1634
-C-N-	-	1357
-C-O	1085	1004
-C=C-	889	-
-C=C-	618	618
Halogen compound	516	523

(200), (220), (222), and (331) planes confirm the face-centred cubic crystalline structure of copper (Figure 8). The results correspond with the reported previous studies [39,43]. However, the XRD pattern exhibited a weak reflection at $\sim 31.65^\circ$ indicating the presence of small amount of Cu_2O which might have occurred due to exposure to open air while transferring into XRD chamber during sample loading. This may be as a result of the metallic CuNPs' extreme sensitivity to oxygen and tendency to easily oxidise [44].

3.5.6. FTIR analysis

The FTIR spectroscopic analysis was carried out to identify the possible biomolecules present in the crude bark extract responsible for capping and reducing copper metal ions into CuNPs. Figure 9 spectra showed the presence of different peaks of biosynthesised CuNPs and *D. indica* bark extract at a different wavelength related to the nature of functional groups. Table 2 demonstrates the functional groups of the phytochemicals present in the *D. indica* bark extract which might help in the capping and stabilisation of CuNPs. A prominent peak found at 1641 cm^{-1} in the *D. indica* bark extract might occur due to the C=C stretching vibration of the aromatic phenols, which was displaced to 1634 cm^{-1} in case of CuNPs suggesting the phenolic compounds interaction with the nanoparticles [35]. Another band at 2368 cm^{-1} in extract indicated the C-H stretching vibrations of $-\text{CH}_3$ groups found in terpenoids and in case of nanoparticle it was shifted to 2128 cm^{-1} . Peak at 1357 cm^{-1} attributed to $-\text{C}-\text{N}$ stretch of aromatic amine [38]. The presence of peak at 3321 cm^{-1} and 3327 cm^{-1} could be due to intermolecular and intramolecular interactions of O-H group in polyphenols or proteins or polysaccharides. Protein-metal

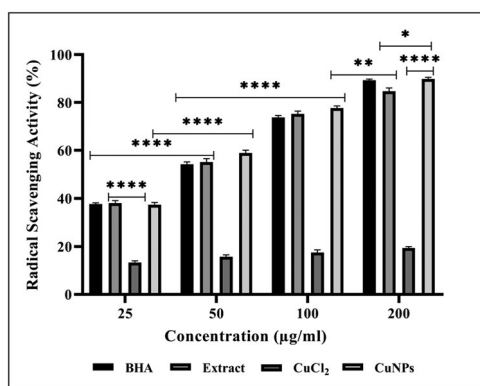


Figure 10. Free radical scavenging activity of BHA, *Dillenia indica* bark extract, CuCl₂ and Cu NPs in concentration-dependent manner. The data represent the mean values of three independent experiments and are presented as mean ± SEM of the absorbance. * $p < 0.05$, ** $p < 0.01$, *** $p < 0.001$ and **** $p < 0.0001$ indicated the significance differences (ANOVA followed by Tukey's Test, $\alpha < 0.05$).

nanoparticles interaction occurs through the unbound amine groups or carboxylate ion of amino acid residues [45]. The peak observed at 1004cm^{-1} attributed to the stretching vibration of C and O bond among alcohol and carboxylic groups [46]. The decreased transmittance observed at 516cm^{-1} in bark extract was shifted to 523cm^{-1} which indicates association of aromatic biomolecules found in the bark extract in the reduction of Cu²⁺ ions. The observation of a common band in the bark extract of *D. indica* and CuNPs suggests the presence of bioactive compounds like terpenoids, phenolics, flavonoids and glycosides on the surface of synthesised CuNPs [12].

3.6. Free radical scavenging activity

One of the basic and simple technique for assessing the radical scavenging capacity of various antioxidant compounds is the DPPH assay [19] using BHA as reference standard. A deep violet free radical, DPPH loses its chromophore and turns yellow when it accepts a proton from any hydrogen donor. Therefore, the degree of discoloration marks the radical scavenging efficiency of sample antioxidants [13]. When biomolecules interact with molecular oxygen in the biological systems, free radicals are produced. These antioxidants suppress the free radical reactions by retarding the initiation step of oxidative chain reactions thereby protecting from cellular damage. Besides that, antioxidants have been regarded as therapeutic agents due to their anti-inflammatory, antitumor, anticancer, anti-mutagenic and antimicrobial properties [47].

In this study, free radical scavenging potential of CuNPs, BHA and *D. indica* bark extract was $89.86\% \pm 0.66$, $89.23\% \pm 0.55$ and $84.73\% \pm 1.33$, respectively (Figure 10). However, the IC₅₀ of CuNPs was found to be lowest, i.e. $37.2\mu\text{g/mL}$ in comparison with extract and BHA which was $56.0\mu\text{g/mL}$ and $66.4\mu\text{g/mL}$, respectively, for inhibition of DPPH radicals. The enhanced antioxidant activity of green synthesised CuNPs could be due to the synergistic effect of both CuNPs and phytochemical substances like phenols and flavonoids present on the surface of nanoparticles, thereby protecting cells from damage caused by free radicals [48]. Analysis of variance clearly showed significant differences at $p < 0.05$ of obtained scavenging activity [21]. A study reported DPPH scavenging activity of *P. austroarabica* synthesised CuNPs showing higher inhibition of 91.82% at $100\mu\text{g/mL}$ [40] which corroborates with the present findings. The enhanced antioxidant activity

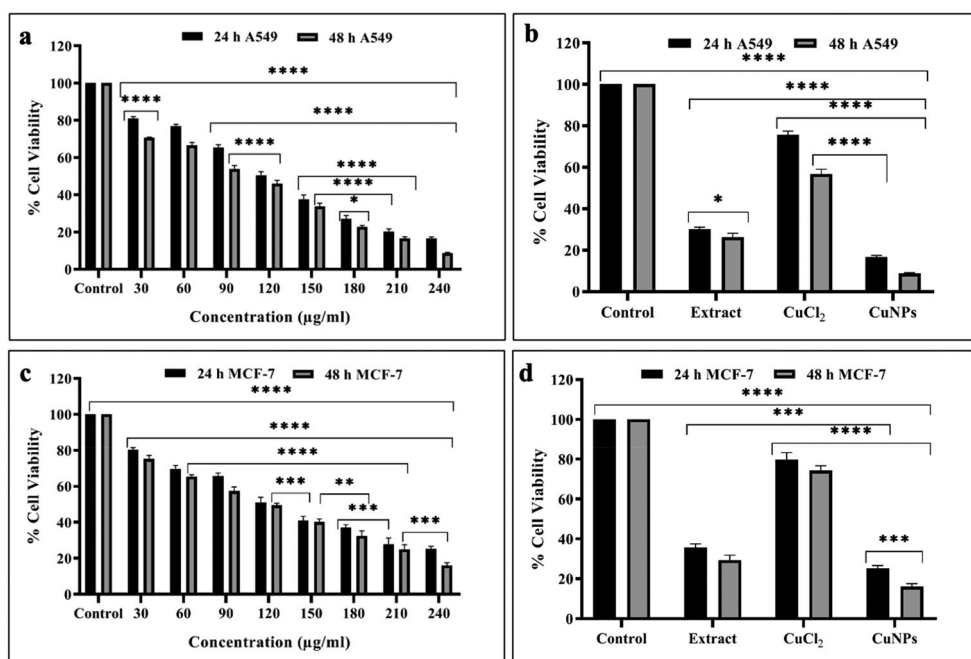


Figure 11. Significant concentration and time-dependent cell viability studies of (a) CuNPs treated A549 cells, (b,d) comparison of cytotoxicity between control, extract, CuCl₂ and CuNPs (c) CuNPs treated MCF-7 cells after 24 and 48 h. Data expressed as mean ± SEM of the absorbance. * $p < 0.05$, ** $p < 0.01$, *** $p < 0.001$ and **** $p < 0.0001$ indicated the significance differences (ANOVA followed by Tukey's Test, $\alpha < 0.05$).

was reported for CuNPs synthesised using *Withania somnifera* root extract with 62% inhibition at 400 µg/mL [41]. Similar study reporting concentration-dependent antioxidant activity of *C. zelanicum* leaf extract-mediated CuNPs were also reported by Liu et al. [49]. Therefore, the findings strongly support the use of bio-fabricated CuNPs as potential antioxidants against numerous oxidative stress-related degenerative diseases.

3.7. Anticancer activity: in vitro

In this study, the anticancer potentials of green synthesised CuNPs were evaluated against human lung cancer cells (A549) and human breast cancer cells (MCF-7) through MTT assay for cell viability, cellular morphology and apoptotic cell death through nuclear staining using AO/EtBr and DAPI dyes.

3.7.1. Cell viability assay

The cell viability of A549 and MCF-7 cell lines treated with CuNPs at different concentrations (0, 30, 60, 90, 120, 150, 180, 210 and 240 µg/mL) for time interval of 24 and 48 h was assessed through MTT assay. The synthesised CuNPs at the concentration of 30 µg/mL showed 81.05% ± 0.575 and 70.68% ± 0.189 viability in 24 and 48 h, respectively, whereas at concentration of 240 µg/mL the cell viability decreased up to 16.68% ± 0.418 and 8.74% ± 0.232 in 24 and 48 h of incubation period respectively in A549 cell lines (Figure 11(a)). Similarly, the treatment of CuNPs affected the cell viability of MCF-7 cell line in dose and time-dependent manner. At 30 µg/mL, the cell viability was 80.20% ± 0.759 and 75.27% ± 1.128 after 24 and 48 h of incubation, respectively, and at 240 µg/mL,

the same parameter was $25.14\% \pm 0.851$ and $16.01\% \pm 0.883$ after 24 and 48 h of incubation, respectively (Figure 11(c)). The results were significantly different ($p < 0.05$) between control and treated groups of A549 and MCF-7 cell lines. As reported by Sankar et al. [52], the extent of cell viability was dose and time-dependent in A549 and MCF-7 cell line treated with CuNPs which corroborates with the findings of this study. The increased cellular toxicity of synthesised CuNPs on both the cell lines in comparison to extract and metal ion solution may be due to the combined effect of the size and increase surface functionalisation of CuNPs with bioactive compounds of *D. indica* bark extract which plays as an encapsulating agent. The anticancer activity of CuNPs has been reported in numerous studies [40,42] and the outcomes obtained in this investigation were consistent with the majority of those previously reported. The cytotoxicity of biosynthesised CuNPs in A549 cell lines was also reported by Harne et al. [50]. Hasanin et al. [26] reported the anticancer efficiency of myco-synthesised CuNPs with IC_{50} at $210 \mu\text{g/mL}$. Concentration and dose-dependent decrease in cell viability was also observed in MCF-7 cell lines treated with CuONPs [51]. Moreover, increasing the concentration of CuNPs and period of incubation time from 24 to 48 h leads to decrease in the number of viable cells which demonstrates the efficiency of the biosynthesised CuNPs in a dose and time-dependent manner.

3.7.2. Nuclear staining

To further support the cytotoxic activities of CuNPs, nuclear staining using dual staining method was carried out to check the plausible mechanistic cell death. Following the evaluation of cell morphology, the induction of apoptosis by nanoparticles in A549 and MCF-7 cells was verified by the differential uptake of fluorescent DNA-binding dyes, such as AO/EtBr. Here, we have used AO/EtBr dual staining method to distinguish the live and dead cells. While EtBr is a membrane-impermeable dye that only stains the DNA of membrane-compromised/dead cells, AO is a membrane-permeable dye that stains both viable and injured cells. As a result, cells stained with AO appear green because their membranes are intact, while cells stained with EtBr (cells devoid of cytoplasm) appear orange or red because of nuclear shrinkage or blebbing. Cells stained with dual dyes have green cytoplasm and yellow-orange nuclei.

Cells were grown in a 96-well plate, and the treatment was carried out as previously indicated. The cells treated with CuNPs ($240 \mu\text{g/mL}$) were found to be greenish yellow at early stage whereas at later stage the apoptotic cells become more concentrated and asymmetrical showing reddish orange in colour due to cell death (Figure 12(a,b)). Sankar et al. [52] treated A549 cells with CuONPs and observed apoptosis induction and orange shattered nuclei compared to control cells. Cell death due to apoptosis was observed through AO/EtBr dual staining of MCF-7 cells exposed to Cu and AgNPs [53]. The control cells without any treatment appear to be green due to intact mitochondrial membrane. The cells treated with extract and metal salt solution as positive control appears as mixture of both live and dead cells. This result correlates with MTT assay results, where we found that there is decrease in number of viable cells in case of extract and CuCl_2 solution. Moreover, the number of membranes blebbed rounded cells increases with increase in incubation time. The degree of apoptotic death of A549 and MCF-7 treated cell line was in the order of $\text{CuNPs} > \text{CuCl}_2 > D. indica$ extract.

3.7.3. DAPI staining

One of the mechanisms used to inhibit cell development is apoptotic cell death. DAPI is a nuclear-specific blue fluorescent dye with a stronger affinity for DNA's A/T-rich sections.

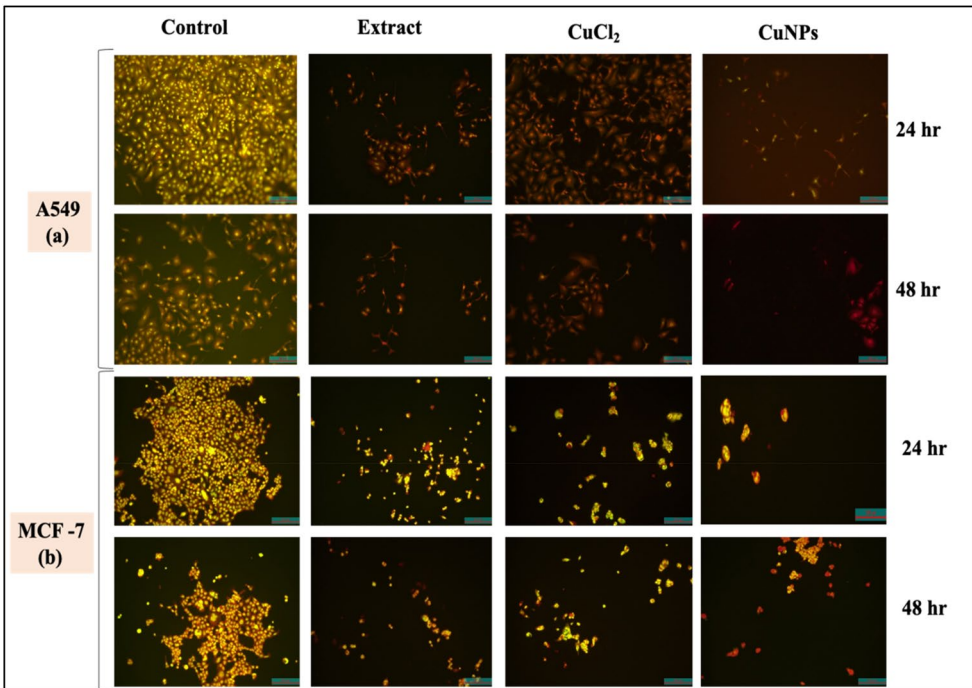


Figure 12. AO/EtBr staining of (a) A549 after 24 and 48h and (b) MCF-7 after 24 and 48h. Images were taken in fluorescence microscope at 10X magnification.

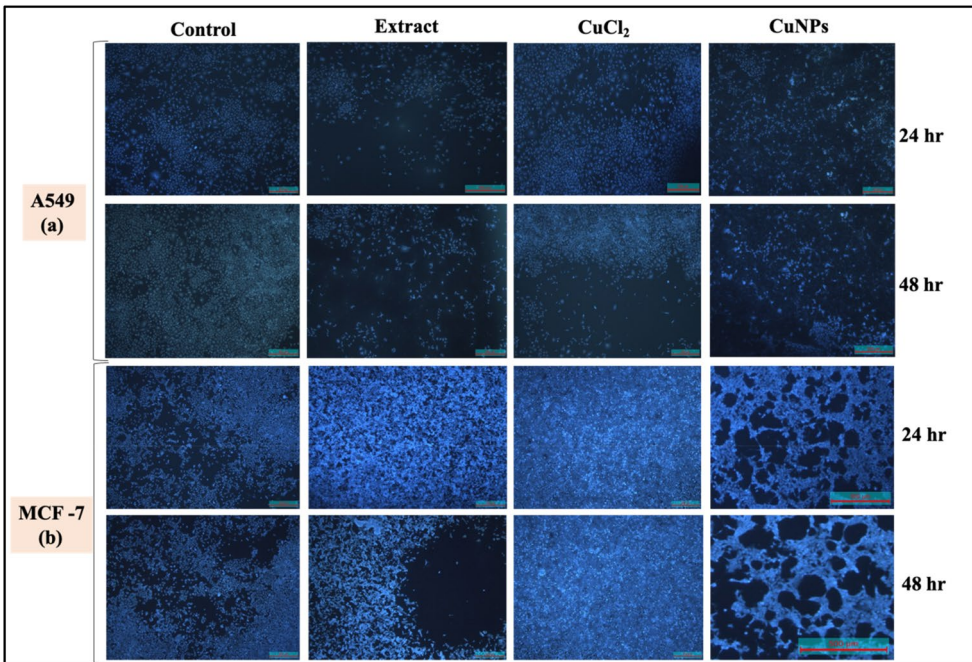


Figure 13. DAPI staining of (a) A549 after 24 and 48h and (b) MCF-7 after 24 and 48h.

This fluorescent tag was used to quantify the proportion of apoptotic cells with condensed and fragmented chromatin as well as to highlight the nuclear alterations that occur during apoptosis [54,55]. From the 24 to 48 h of CuNPs treatment, the nuclear morphological analyses revealed a rise in the number of cells with small, condensed nuclei, indicating a growing number of apoptotic cells with increasing period of incubation (Figure 13(a,b)). Apart from nuclear condensation, the stained cells appeared to lose their structure with the increasing incubation period from 24 to 48 h. The numbers of apoptotic cells were significantly higher in CuNPs treated groups as compared to control cells. The control cells tend to maintain their shape and size. Thus, this staining revealed the morphological changes in CuNPs treated cells in terms of both DNA disintegration and chromatin condensation. Baharara et al. [56] observed the DNA fragmentation in MCF-7 cells treated with biosynthesised AgNPs using DAPI fluorescent stain.

3.7.4. Putative mechanistic insight to cytotoxicity

Absorption of metal nanoparticles into the systemic circulation of human body mainly depends upon their physicochemical properties which contribute to potential toxicity at specific target site. From the recent findings, it was observed that biosynthesised CuNPs have potential cytotoxic efficiency against both A549 and MCF-7 cell lines. Numerous studies have reported the cytotoxic effect of plant-mediated CuNPs against different cell lines. However, the exact signalling mechanism underlying cytotoxicity is still evolving. Based on the present findings and observations a probable schematic mechanistic input has been represented to understand the cause and effect of CuNPs induced cytotoxicity (Figure 14).

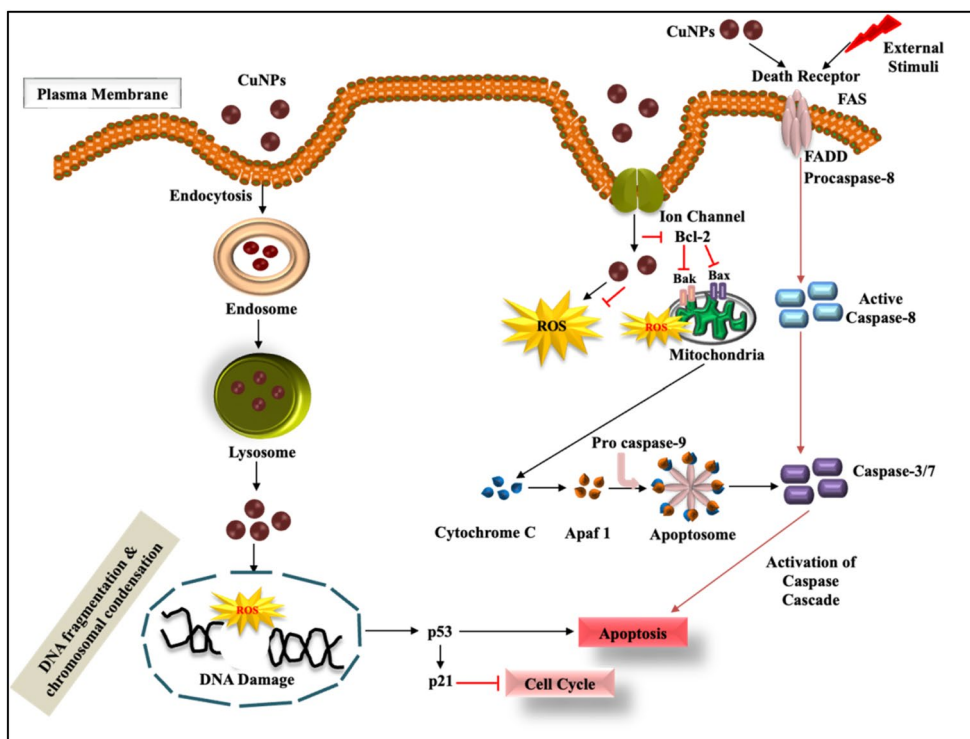


Figure 14. Schematic illustration of the cytotoxic potency of plant-mediated CuNPs.

According to different literature survey, generation of reactive oxygen species (ROS) has been considered as one of the major causes of toxicity *in vitro* induced by phyto-mediated nanoparticles. The mechanism of action mainly lies with either direct interaction of CuNPs with the surface of the cancer cells after exposure or by dissolution of metal ions thus, inducing oxidative stress. Therefore, in order to reduce the toxic impact of metal ions released from NPs the capping of NPs is done with biological reducers which showed greater stability and cytotoxicity towards cancer cells *in vitro* [57]. Thus, the green method of synthesising CuNPs could be considered safe for its use as cancer therapeutics.

It has been reported that cells undergo trillions of oxidative hits per day. Controlled generation of ROS helps to maintain controlled cellular proliferation and differentiation. But for some reason if the ROS levels increase (due to aerobic glycolysis) or scavenged ROS decrease, then the cells undergo a certain condition called oxidative stress [58]. Excessive intracellular ROS production may cause DNA damage (attributed to DNA fragmentation), cell cycle arrest, apoptosis, cytotoxicity, genotoxicity and alterations in cellular motility. In addition, ROS oxidises DNA and RNA's complementary bases, which results in genetic mutations and organism damage [59]. However, alterations in DNA leads to overexpression of tumour suppressor genes, i.e. p53 and p21 which in turn induces apoptosis and inhibits cell cycle [60]. Synthesis of CuO NPs using *E. globulus* leaf extract and *Beta vulgaris* extract inhibits cell cycle at G2/M phase in MCF-7 and A549 cancer cells, respectively [61]. The ROS-induced toxicity depends on shape, size and chemical composition of CuNPs. Small-sized NPs have large surface to volume ratio which leads to greater ROS formation inducing cytotoxicity [26].

ROS-induced programmed cell death is initiated by cysteine-dependent proteases called caspases. Apoptosis involves intrinsic and extrinsic pathways which lead to formation of apoptotic bodies that are finally removed by neighbouring phagocytes [62]. The intrinsic pathway implies activation of proapoptotic proteins Bak/Bax expression on mitochondrial membrane followed by Bcl-2 induced membrane permeabilisation and liberation of cytochrome c into the cytoplasm. This cyt-c combines with procaspase-9 and Apaf-1 adaptor to form apoptosome which further instigates caspase cascade pathway causing apoptosis [63]. Extrinsic pathway involves interaction of death ligand-receptor on the cell surface for activation of caspase-8. Further activation of executioner caspases 3 and 7 leads to cleavage of proteins and cytoskeleton causing cell death. Dey et al. [64] reported the upregulation of intrinsic and extrinsic protein such as Bax, cyt-c, caspase 7/9 and caspase 8 in CuONPs treated MCF-7 and HeLa cell lines implying efficiency to initiate apoptosis.

Taking to the fact, CuNPs exert toxicity on cancer cell lines through various signalling methods including ROS generation, programmed cell death, antioxidant activity, cell cycle arrest, etc. The mode of action of plant extract synthesised CuNPs mainly depend upon the potential route of uptake, source and translocation pathways of Cu NPs and the type of cell line used for study. Therefore, it is important to understand the molecular mechanism as well as its effects in order to provide better input in the field of biomedicine.

4. Conclusion

Dillenia indica is an underutilised plant valued for its medicinal uses and constitutes bio-active phytochemicals. This study reported for the first time to synthesise CuNPs using ethanolic bark extract of *Dillenia indica* as bio-reductant. Such synthesised CuNPs were

crystalline, spherical in shape, well dispersed and possessed a highly negative zeta potential value -41.8 mV with a stability up to one month as observed. It appears that the phytoconstituents of *D. indica* bark extract were responsible for bio-reduction process during the synthesis of CuNPs and also act as capping agents to stabilise the CuNPs. FESEM image showed that the average size of CuNPs was 35.43 nm along with EDX analysis indicating the presence of elemental copper. Synthesised CuNPs illustrated strong free radical scavenging activity as evaluated by DPPH assay. Moreover, the cytotoxicity of CuNPs, CuCl_2 and extract was compared and analysed through MTT assay in dose and concentration-dependent manner in A549 and MCF-7 cancer cells. Nuclear fluorescent staining by AO/EtBr and DAPI dyes indicates CuNPs induced apoptotic-related cytomorphological alterations in both the cell lines. In brief, this study portrayed the potent free radical scavenging and specific cytotoxic potential of biosynthesised CuNPs against cancer cells making it as an effective tool in the field of nanomedicine.

Acknowledgments

The authors acknowledge the Director, CSIR-IMMT, Bhubaneswar, Odisha for his constant support and encouragement. The authors are further thankful to Imgenex, Bhubaneswar, India for providing cell lines to conduct the experiment. Ms. Larica Mohanta also gratefully thanks CSIR-HRDG, Govt. of India for awarding CSIR-NET Junior Research Fellowship (File No: 31/009(0151)/2019-EMR-I).

Disclosure statement

There are no conflicts of interest to declare, including any financial, personal or other relationship with other people or organisations.

Notes on contributors

Ms. Larica Mohanta has completed her Master's degree in Zoology from CBSH-OUAT, Bhubaneswar. She obtained her MPhil degree in zoology from Ravenshaw University, Cuttack. She qualified CSIR-NET JRF in life science and currently she is pursuing her Ph.D. degree as CSIR-SRF fellow at CSIR-IMMT, Bhubaneswar, India. Her research work is based on toxicity of metal nanoparticles synthesized from plant extracts and its biological applications in cellular and animal models.

Dr. Bhabani Sankar Jena has obtained his Ph.D. degree in Zoology from Berhampur University, Odisha, India with specialization in Cell Physiology & Biochemistry. He is working as Chief Scientist in Project Monitoring & Evaluation Department at CSIR-IMMT, Bhubaneswar, India. His research interests include experimental gerontology, food Science and technology, bioactive compounds from natural sources and nanotoxicology. His research publications include 43 journal articles in high impact factor journals. He has also published book chapters and received 14 patents (national and international).

Data availability

All data that support the findings of this study have been included in the article.

References

1. Tauran Y, Brioude A, Coleman AW, et al. Molecular recognition by gold, silver and copper nanoparticles. *World J Biol Chem.* 2013;4(3):1–23. doi: [10.4331/wjbc.v4.i3.35](https://doi.org/10.4331/wjbc.v4.i3.35).
2. Narayanan KB, Sakthivel N. Biological synthesis of metal nanoparticles by microbes. *Adv Colloid Interface Sci.* 2010;156(1–2):1–13. doi: [10.1016/j.cis.2010.02.001](https://doi.org/10.1016/j.cis.2010.02.001).
3. Remya RR, Rajasree SRR, Aranganathan L, et al. An investigation on cytotoxic effect of bioactive AgNPs synthesized using *cassia fistula* flower extract on breast cancer cell MCF-7. *Biotechnol Rep (Amst).* 2015;8:110–115. doi: [10.1016/j.btre.2015.10.004](https://doi.org/10.1016/j.btre.2015.10.004).

4. Makarov VV, Love AJ, Sinityna OV, et al. "Green" nanotechnologies: synthesis of metal nanoparticles using plants. 2014;6(1):35–44. doi: [10.32607/20758251-2014-6-1-35-44](https://doi.org/10.32607/20758251-2014-6-1-35-44).
5. Noruzi M. Biosynthesis of gold nanoparticles using plant extracts. *Bioprocess Biosyst Eng*. 2015;38(1):1–14. doi: [10.1007/s00449-014-1251-0](https://doi.org/10.1007/s00449-014-1251-0).
6. Mott D, Galkowski J, Wang L, et al. Synthesis of size-controlled and shaped copper nanoparticles. *Langmuir*. 2007;23(10):5740–5745. doi: [10.1021/la0635092](https://doi.org/10.1021/la0635092).
7. Shi B, Yuan Y, Jin M, et al. Transcriptomic and physiological analyses of hepatopancreas reveal the key metabolic changes in response to dietary copper level in pacific white shrimp *Litopenaeus vannamei*. *Aquaculture*. 2021;532:736060. doi: [10.1016/j.aquaculture.2020.736060](https://doi.org/10.1016/j.aquaculture.2020.736060).
8. Adewale Akintelu S, Kolawole Oyebamiji A, Charles Olugbeko S, et al. Green chemistry approach towards the synthesis of copper nanoparticles and its potential applications as therapeutic agents and environmental control. *Curr Res Green Sustain Chem*. 2021;4:100176. doi: [10.1016/j.crgsc.2021.100176](https://doi.org/10.1016/j.crgsc.2021.100176).
9. Park BK, Jeong S, Kim D, et al. Synthesis and size control of monodisperse copper nanoparticles by polyol method. *J Colloid Interface Sci*. 2007;311(2):417–424. doi: [10.1016/j.jcis.2007.03.039](https://doi.org/10.1016/j.jcis.2007.03.039).
10. Kumar V, Kumar S, Kumar V. Antidiabetic and antihyperlipidemic effects of *dillenia indica* (L.) leaves extract. *Braz J Pharm Sci*. 2011;47(2):373–378. doi: [10.1590/S1984-82502011000200018](https://doi.org/10.1590/S1984-82502011000200018).
11. Deepa N, Jena BS. Antioxidant fraction from bark of *Dillenia indica*. *Int J Food Prop*. 2011;14(5):1152–1159. doi: [10.1080/10942911003592779](https://doi.org/10.1080/10942911003592779).
12. Parvin MN, Rahman MS, Islam MS, et al. Chemical and biological investigations of *dillenia indica* Linn. *Bangladesh J Pharmacol*. 2009;4:122–125.
13. Mohanty AS, Jena BS. Innate catalytic and free radical scavenging activities of silver nanoparticles synthesized using *dillenia indica* bark extract. *J Colloid Interface Sci*. 2017;496:513–521. doi: [10.1016/j.jcis.2017.02.045](https://doi.org/10.1016/j.jcis.2017.02.045).
14. Alahmdi MI, Khasim S, Vanaraj S, et al. Green nanoarchitectonics of ZnO nanoparticles from *Clitoria ternatea* flower extract for in vitro anticancer and antibacterial activity: inhibits MCF-7 cell proliferation via intrinsic apoptotic pathway. *J Inorg Organomet Polym*. 2022;32(6):2146–2159. doi: [10.1007/s10904-022-02263-7](https://doi.org/10.1007/s10904-022-02263-7).
15. Torre LA, Siegel RL, Jemal A. Lung cancer statistics. *Adv Exp Med Biol*. 2016;893:1–19.
16. Ferlay J, Soerjomataram I, Dikshit R, et al. Cancer incidence and mortality worldwide: sources, methods and major patterns in GLOBOCAN 2012. *Int J Cancer*. 2015;136(5):E359–E386. doi: [10.1002/ijc.29210](https://doi.org/10.1002/ijc.29210).
17. Thun M, Peto R, Boreham J, et al. Stages of the cigarette epidemic on entering its second century. *Tob Control*. 2012;21(2):96–101. doi: [10.1136/tobaccocontrol-2011-050294](https://doi.org/10.1136/tobaccocontrol-2011-050294).
18. Singh D, Kumar V, Yadav E, et al. One-pot green synthesis and structural characterisation of silver nanoparticles using aqueous leaves extract of *Carissa carandas*: antioxidant, anticancer and antibacterial activities. *IET Nanobiotechnol*. 2018;12(6):748–756. doi: [10.1049/iet-nbt.2017.0261](https://doi.org/10.1049/iet-nbt.2017.0261).
19. Akther T, Mathipi V, Kumar NS, et al. Fungal-mediated synthesis of pharmaceutically active silver nanoparticles and anticancer property against A549 cells through apoptosis. *Environ Sci Pollut Res Int*. 2019;26:13649–13657. doi: [10.1007/s11356-019-04718-w](https://doi.org/10.1007/s11356-019-04718-w).
20. Vairavel M, Devaraj E, Shanmugam R. An eco-friendly synthesis of enterococcus sp.-mediated gold nanoparticle induces cytotoxicity in human colorectal cancer cells. *Environ Sci Pollut Res Int*. 2020;27(8):8166–8175. doi: [10.1007/s11356-019-07511-x](https://doi.org/10.1007/s11356-019-07511-x).
21. Shwetha UR, Latha MS, Rajith Kumar CR, et al. Facile synthesis of zinc oxide nanoparticles using novel *areca catechu* leaves extract and their in vitro antidiabetic and anticancer studies. *J Inorg Organomet Polym*. 2020;30(12):4876–4883. doi: [10.1007/s10904-020-01575-w](https://doi.org/10.1007/s10904-020-01575-w).
22. Valodkar M, Jadeja RN, Thounaojam MC, et al. Biocompatible synthesis of peptide capped copper nanoparticles and their biological effect on tumor cells. *Mater Chem Phys*. 2011;128(1–2):83–89. doi: [10.1016/j.matchemphys.2011.02.039](https://doi.org/10.1016/j.matchemphys.2011.02.039).
23. Chung I, Rahuman AA, Marimuthu S, et al. Green synthesis of copper nanoparticles using *Eclipta prostrata* leaves extract and their antioxidant and cytotoxic activities. *Exp Ther Med*. 2017;14:18–24.
24. Elemike EE, Onwudiwe DC, Singh M. Eco-friendly synthesis of copper oxide, zinc oxide and copper oxide–zinc oxide nanocomposites, and their anticancer applications. *J Inorg Organomet Polym*. 2020;30(2):400–409. doi: [10.1007/s10904-019-01198-w](https://doi.org/10.1007/s10904-019-01198-w).
25. Manikandan DB, Arumugam M, Veeran S, et al. Biofabrication of ecofriendly copper oxide nanoparticles using *Ocimum americanum* aqueous leaf extract: analysis of in vitro antibacterial, anticancer, and photocatalytic activities. *Environ Sci Pollut Res Int*. 2021;28(26):33927–33941. doi: [10.1007/s11356-020-12108-w](https://doi.org/10.1007/s11356-020-12108-w).
26. Hasanin M, Al Abboud MA, Alawlaqi MM, et al. Ecofriendly synthesis of biosynthesized copper nanoparticles with Starch-Based nanocomposite: antimicrobial, antioxidant, and anticancer activities. *Biol Trace Elem Res*. 2022;200(5):2099–2112. doi: [10.1007/s12011-021-02812-0](https://doi.org/10.1007/s12011-021-02812-0).

27. Rehana D, Mahendiran D, Kumar RS, et al. Evaluation of antioxidant and anticancer activity of copper oxide nanoparticles synthesized using medicinally important plant extracts. *Biomed Pharmacother.* 2017;89:1067–1077. doi: [10.1016/j.biopha.2017.02.101](https://doi.org/10.1016/j.biopha.2017.02.101).
28. Senthilkumar N, Nandhakumar E, Priya P, et al. Synthesis of ZnO nanoparticles using leaf extract of: *Tectona grandis* (L.) and their anti-bacterial, anti-arthritis, anti-oxidant and in vitro cytotoxicity activities. *New J Chem.* 2017;41(18):10347–10356. doi: [10.1039/C7NJ02664A](https://doi.org/10.1039/C7NJ02664A).
29. Dutta T, Paul A, Majumder M, et al. Pharmacological evidence for the use of *Cissus assamica* as a medicinal plant in the management of pain and pyrexia. *Biochem Biophys Rep.* 2020;21:100715.
30. Kiran MS, Betageri VS, Kumar CRR, et al. In-Vitro antibacterial, antioxidant and cytotoxic potential of silver nanoparticles synthesized using novel *Eucalyptus tereticornis* leaves extract. *J Inorg Organomet Polym.* 2020;30(8):2916–2925. doi: [10.1007/s10904-020-01443-7](https://doi.org/10.1007/s10904-020-01443-7).
31. Kntayya SB, Ibrahim MD, Ain NM, et al. Induction of apoptosis and cytotoxicity by isothiocyanate sulforaphene in human hepatocarcinoma HepG2 cells. *Nutrients.* 2018;10:718. doi: [10.3390/nu10060718](https://doi.org/10.3390/nu10060718).
32. Weng X, Guo M, Luo F, et al. One-step green synthesis of bimetallic Fe/Ni nanoparticles by eucalyptus leaf extract: biomolecules identification, characterization and catalytic activity. *Chem Eng J.* 2017;308:904–911. doi: [10.1016/j.cej.2016.09.134](https://doi.org/10.1016/j.cej.2016.09.134).
33. Din MI, Arshad F, Hussain Z, et al. Green adeptness in the synthesis and stabilization of copper nanoparticles: catalytic, antibacterial, cytotoxicity, and antioxidant activities. *Nanoscale Res Lett.* 2017;12:638. doi: [10.1186/s11671-017-2399-8](https://doi.org/10.1186/s11671-017-2399-8).
34. Nagar N, Devra V. Green synthesis and characterization of copper nanoparticles using *Azadirachta indica* leaves. *Mater Chem Phys.* 2018;213:44–51. doi: [10.1016/j.matchemphys.2018.04.007](https://doi.org/10.1016/j.matchemphys.2018.04.007).
35. Kiruba Daniel SCG, Vinothini G, Subramanian N, et al. Biosynthesis of Cu, ZVI, and Ag nanoparticles using *Dodonaea viscosa* extract for antibacterial activity against human pathogens. *J Nanopart Res.* 2013;15(1):1319. doi: [10.1007/s11051-012-1319-1](https://doi.org/10.1007/s11051-012-1319-1).
36. Vaseem M, Lee KM, Kim DY, et al. Parametric study of cost-effective synthesis of crystalline copper nanoparticles and their crystallographic characterization. *Mater Chem Phys.* 2011;125(3):334–341. doi: [10.1016/j.matchemphys.2010.11.007](https://doi.org/10.1016/j.matchemphys.2010.11.007).
37. Yallappa S, Manjanna J, Sindhe MA, et al. Microwave assisted rapid synthesis and biological evaluation of stable copper nanoparticles using *T. arjuna* bark extract. *Spectrochim Acta A Mol Biomol Spectrosc.* 2013;110:108–115. doi: [10.1016/j.saa.2013.03.005](https://doi.org/10.1016/j.saa.2013.03.005).
38. Momeni SS, Nasrollahzadeh M, Rustaiyan A. Green synthesis of the Cu/ZnO nanoparticles mediated by *Euphorbia prolifera* leaf extract and investigation of their catalytic activity. *J Colloid Interface Sci.* 2016;472:173–179. doi: [10.1016/j.jcis.2016.03.042](https://doi.org/10.1016/j.jcis.2016.03.042).
39. Gu J, Aidy A, Goorani S. Anti-human lung adenocarcinoma, cytotoxicity, and antioxidant potentials of copper nanoparticles green-synthesized by *calendula officinalis*. *J Exp Nanosci.* 2022;17(1):285–296. doi: [10.1080/17458080.2022.2066082](https://doi.org/10.1080/17458080.2022.2066082).
40. Alahdal FAM, Qashqoosh MTA, Manea YK, et al. Green synthesis and characterization of copper nanoparticles using *Phragmanthera austroarabica* extract and their biological/environmental applications. *Sustain Mater Technol.* 2023;35:e00540. doi: [10.1016/j.susmat.2022.e00540](https://doi.org/10.1016/j.susmat.2022.e00540).
41. Shanmugapriya J, Reshma CA, Srinidhi V, et al. Green synthesis of copper nanoparticles using *Withania somnifera* and its antioxidant and antibacterial activity. *J Nanomater.* 2022;2022:1–9. doi: [10.1155/2022/7967294](https://doi.org/10.1155/2022/7967294).
42. Jahan I, Erci F, Isildak I. Facile microwave-mediated green synthesis of non-toxic copper nanoparticles using *citrus sinensis* aqueous fruit extract and their antibacterial potentials. *J Drug Deliv Sci Technol.* 2021;61:102172. doi: [10.1016/j.jddst.2020.102172](https://doi.org/10.1016/j.jddst.2020.102172).
43. Khani R, Roostaei B, Bagherzade G, et al. Green synthesis of copper nanoparticles by fruit extract of *Ziziphus spina-christi* (L.) willd.: application for adsorption of triphenylmethane dye and antibacterial assay. *J Mol Liq.* 2018;255:541–549. doi: [10.1016/j.molliq.2018.02.010](https://doi.org/10.1016/j.molliq.2018.02.010).
44. Rice KP, Walker EJ, Stoykovich MP, et al. Solvent-dependent surface plasmon response and oxidation of copper nanocrystals. *J Phys Chem C.* 2011;115(5):1793–1799. doi: [10.1021/jp110483z](https://doi.org/10.1021/jp110483z).
45. Gondwal M, Joshi Nee Pant G. Synthesis and catalytic and biological activities of silver and copper nanoparticles using *cassia occidentalis*. *Int J Biomater.* 2018;2018:6735426. doi: [10.1155/2018/6735426](https://doi.org/10.1155/2018/6735426).
46. Ahmed A, Usman M, Liu QY, et al. Plant mediated synthesis of copper nanoparticles by using *camelia sinensis* leaves extract and their applications in dye degradation. *Ferroelectrics.* 2019;549(1):61–69. doi: [10.1080/00150193.2019.1592544](https://doi.org/10.1080/00150193.2019.1592544).
47. Tinggi U. Selenium: its role as antioxidant in human health. *Environ Health Prev Med.* 2008;13(2):102–108. doi: [10.1007/s12199-007-0019-4](https://doi.org/10.1007/s12199-007-0019-4).

48. Demirci Gültekin D, Alaylı Güngör A, Önem H, et al. Synthesis of copper nanoparticles using a different method: determination of its antioxidant and antimicrobial activity. *J Turk Chem Soc A Chem.* 2016;3(3):623–623. doi: [10.18596/jotcsa.287299](https://doi.org/10.18596/jotcsa.287299).
49. Liu H, Wang G, Liu J, et al. Green synthesis of copper nanoparticles using *Cinnamomum zelanicum* extract and its applications as a highly efficient antioxidant and anti-human lung carcinoma. *J Exp Nanosci.* 2021;16:411–423.
50. Harne S, Sharma A, Dhaygude M, et al. Novel route for rapid biosynthesis of copper nanoparticles using aqueous extract of *Calotropis procera* L. latex and their cytotoxicity on tumor cells. *Colloids Surf B Biointerfaces.* 2012;95:284–288. doi: [10.1016/j.colsurfb.2012.03.005](https://doi.org/10.1016/j.colsurfb.2012.03.005).
51. Siddiqui MA, Wahab R, Ahmad J, et al. Single and multi-metal oxide nanoparticles induced cytotoxicity and ROS generation in human breast cancer (MCF-7) cells. *J Inorg Organomet Polym.* 2020;30(10):4106–4116. doi: [10.1007/s10904-020-01564-z](https://doi.org/10.1007/s10904-020-01564-z).
52. Sankar R, Maheswari R, Karthik S, et al. Anticancer activity of *Ficus religiosa* engineered copper oxide nanoparticles. *Mater Sci Eng C Mater Biol Appl.* 2014;44:234–239. doi: [10.1016/j.msec.2014.08.030](https://doi.org/10.1016/j.msec.2014.08.030).
53. Solairaj D, Rameshthangam P, Arunachalam G. Anticancer activity of silver and copper embedded chitin nanocomposites against human breast cancer (MCF-7) cells. *Int J Biol Macromol.* 2017;105(Pt 1):608–619. doi: [10.1016/j.ijbiomac.2017.07.078](https://doi.org/10.1016/j.ijbiomac.2017.07.078).
54. Choi BY, Kim HY, Lee KH, et al. Clo^olium, a potassium channel blocker, induces apoptosis of human promyelocytic leukemia (HL-60) cells via Bcl-2-insensitive activation of caspase-3. Available from: www.elsevier.com/locate/canlet
55. Sreelatha S, Jeyachitra A, Padma PR. Antiproliferation and induction of apoptosis by *Moringa oleifera* leaf extract on human cancer cells. *Food Chem Toxicol.* 2011;49(6):1270–1275. doi: [10.1016/j.fct.2011.03.006](https://doi.org/10.1016/j.fct.2011.03.006).
56. Baharara J, Namvar F, Ramezani T, et al. Silver nanoparticles biosynthesized using *Achillea biebersteinii* flower extract: apoptosis induction in MCF-7 cells via caspase activation and regulation of bax and bcl-2 gene expression. *Molecules.* 2015;20(2):2693–2706. doi: [10.3390/molecules20022693](https://doi.org/10.3390/molecules20022693).
57. Perreault F, Popovic R, Dewez D. Different toxicity mechanisms between bare and polymer-coated copper oxide nanoparticles in *Lemna gibba*. *Environ Pollut.* 2014;185:219–227. doi: [10.1016/j.envpol.2013.10.027](https://doi.org/10.1016/j.envpol.2013.10.027).
58. Perillo B, Di Donato M, Pezone A, et al. ROS in cancer therapy: the bright side of the moon. *Exp Mol Med.* 2020;52:192–203. doi: [10.1038/s12276-020-0384-2](https://doi.org/10.1038/s12276-020-0384-2).
59. Buchman JT, Hudson-Smith NV, Landy KM, et al. Understanding nanoparticle toxicity mechanisms to inform redesign strategies to reduce environmental impact. *Acc Chem Res.* 2019;52(6):1632–1642. doi: [10.1021/acs.accounts.9b00053](https://doi.org/10.1021/acs.accounts.9b00053).
60. Letchumanan D, Sok SPM, Ibrahim S, et al. Plant-based biosynthesis of copper/copper oxide nanoparticles: an update on their applications in biomedicine, mechanisms, and toxicity. *Biomolecules.* 2021;11:564. doi: [10.3390/biom11040564](https://doi.org/10.3390/biom11040564).
61. Chandrasekaran R, Yadav SA, Sivaperumal S. Phytosynthesis and characterization of copper oxide nanoparticles using the aqueous extract of *Beta vulgaris* L and evaluation of their antibacterial and anticancer activities. *J Clust Sci.* 2020;31(1):221–230. doi: [10.1007/s10876-019-01640-6](https://doi.org/10.1007/s10876-019-01640-6).
62. Chandra J, Samali A, Orrenius S. Triggering and modulation of apoptosis by oxidative stress. *Free Radic Biol Med.* 2000;29(3–4):323–333. doi: [10.1016/s0891-5849\(00\)00302-6](https://doi.org/10.1016/s0891-5849(00)00302-6).
63. Pfeffer CM, Singh ATK. Apoptosis: a target for anticancer therapy. *Int J Mol Sci.* 2018;19:448. doi: [10.3390/ijms19020448](https://doi.org/10.3390/ijms19020448).
64. Dey A, Manna S, Chattopadhyay S, et al. *Azadirachta indica* leaves mediated green synthesized copper oxide nanoparticles induce apoptosis through activation of TNF- α and caspases signaling pathway against cancer cells. *J Saudi Chem Soc.* 2019;23(2):222–238. doi: [10.1016/j.jscs.2018.06.011](https://doi.org/10.1016/j.jscs.2018.06.011).